Inorganic Chemistry

ARTICLE

pubs.acs.org/IC

Coordination Mode Dependent Excited State Behavior in Group 8 Phosphino(terthiophene) Complexes

Stephanie A. Moore,[†] Jeffrey K. Nagle,[‡] Michael O. Wolf,*[,†] and Brian O. Patrick[†]

[†]Department of Chemistry, University of British Columbia, Vancouver, British Columbia V6T 1Z1, Canada

[‡]Department of Chemistry, Bowdoin College, Brunswick, Maine 04011, United States

Supporting Information

ABSTRACT: The ground and excited state behavior of four Ru(II) and Os(II) bipyridyl complexes containing the 3′-(diphenylphosphino)-2,2′:5′,2″-terthiophene (PT_3) ligand in two different coordination modes (*P,S* and *P,C*) is reported. The complexes are generally stable under extended photoirradiation, except for $[Ru(bpy)_2PT_3$-*P,S*$](PF_6)_2$ which decomposes. Emission lifetimes and transient absorption spectra and lifetimes have been obtained for all the complexes. These data support a PT_3 ligand based lowest excited state in the case of both *P,S* bound complexes, and a charge separated lowest excited state in both *P,C* bound complexes, conclusions supported by Density Functional Theory (DFT) calculations.

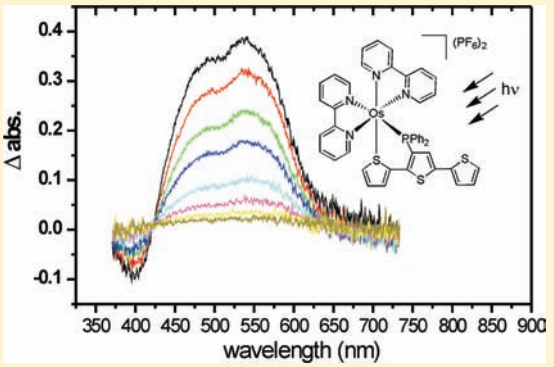

INTRODUCTION

Group 8 polypyridyl complexes have been widely studied as photosensitizing dyes for solar energy harvesting because of their chemical stability, absorbance, and emission properties, and their ability to participate in electron and energy transfer processes.[1,2] In the dye-sensitized solar cell (DSSC) pioneered by Grätzel and O'Regan,[3] electron injection into a wide bandgap semiconductor from such dyes is central to absorption of solar light and charge separation. Conjugated oligomers and polymers are another class of materials that are being investigated for application as light absorbers in organic solar cells.[4,5] The efficiency of cells based on these materials is typically limited by exciton recombination on the conjugated chains.[6] A different approach involves coupling a light absorbing metal dye to a conjugated backbone, with the goal of exciting an electron from the conjugated group to a peripheral ligand on the metal complex generating a charge-separated excited state. This approach offers the possibility of hole transport over longer distances via the π-conjugated backbone. However, energy transfer to competing, low-lying states can present complications.[7,8]

When metal complexes are coordinated to conjugated oligomers and polymers, interactions occur which modify the physical, chemical, and electronic properties of both species.[9] Metals can be incorporated into conjugated materials, such as oligothiophenes or polythiophenes, by direct insertion into the chain,[9,10] direct bonding to the backbone through a thiophene,[11] bipyridyl,[12] or other group, or as pendant groups attached directly through a ligand.[13] The coordination mode can have a significant effect on the excited state interactions. We have previously shown that the ground and excited state behavior of

Chart 1

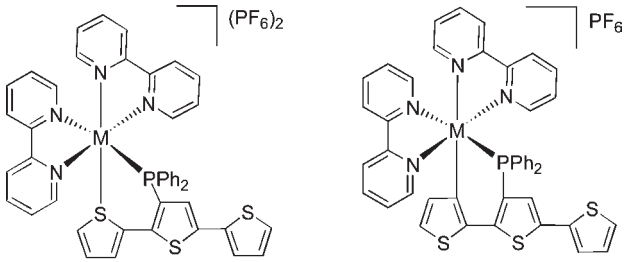

1 M = Ru
3 M = Os

2 M = Ru
4 M = Os

the Ru(II) bis(bipyridyl) complexes[14,15] **1** and **2**, where a terthiophene is tethered to the metal through a diphenylphosphine ligand (Chart 1) via either *P,C* or *P,S* coordination, differ significantly from each other. Visible light excitation of an analogue of complex **2**, in which the conjugation in the phosphino(oligothiophene) ligand is extended to five thiophene rings, resulted in a transient species assigned as a charge-separated excited state.[16] Others have recently explored the utility of cyclometalated complexes as dyes in DSSCs,[17,18] raising the possibility that cyclometalated complexes such as **2** may find application in these types of cells. The possible presence of low-lying metal-centered (MC) excited states[8] or low-lying

Received: February 24, 2011
Published: May 02, 2011

Scheme 1

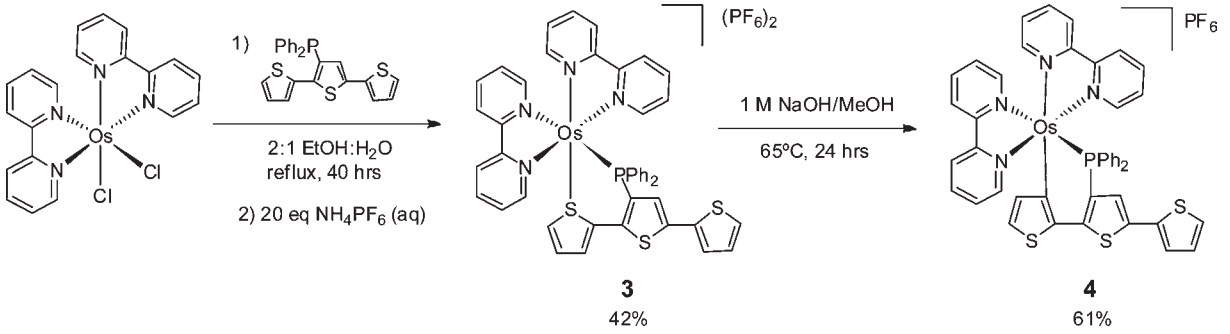

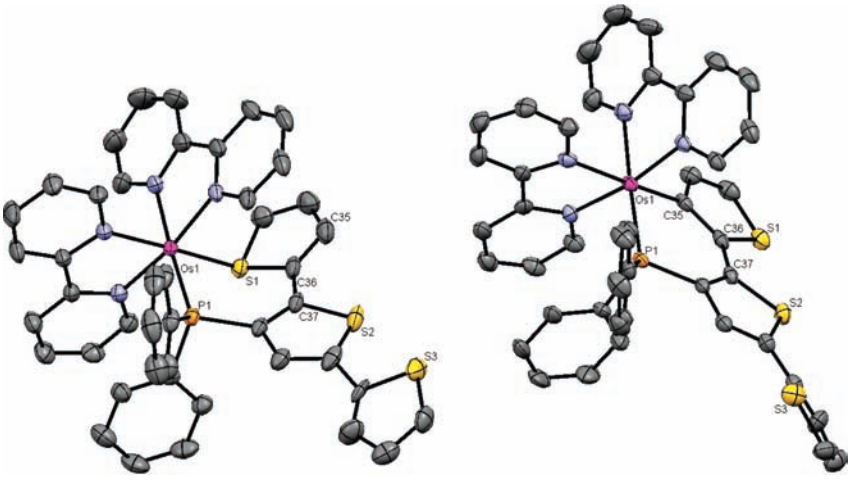

Figure 1. Solid state structures of $[Os(bpy)_2PT_3\text{-}P,S](PF_6)_2$ (**3**) (left) and $[Os(bpy)_2PT_3\text{-}P,C](PF_6)$ (**4**) (right). Hydrogen atoms, counterions, and solvent in lattice removed for clarity. Thermal ellipsoids are drawn at 50% probability.

ligand-based triplet states[7] which can be populated from the metal-to-ligand charge transfer (MLCT) state may lead to alternate routes for deactivation of the excited state in these Ru complexes. Os(II) has a larger ligand field splitting energy (by about ~30%) than Ru which results in an increased energy gap between MLCT and MC states,[8] thus Os(II) analogues of the Ru(II) complexes **1** and **2** may have longer charge-separated lifetimes. On the other hand, some Os(II) polypyridyl complexes have been shown to have shorter excited state lifetimes than the analogous Ru(II) complexes because of enhanced spin−orbit coupling.[19] In cases where ligands with a triplet state close in energy to the ^{3}MLCT state are present, energy transfer between the two states may occur.[20] Os(II) polypyridyl complexes also typically have lower energy MLCT states, leading to broader absorption of light over more of the visible spectrum. This is an advantage for solar energy harvesting where low energy photons must also be captured for maximum efficiency. Here, we report two new Os(II) complexes (**3** and **4**) with conjugated terthiophene based ligands, and compare their photophysical and excited state electronic properties to the Ru(II) analogues.

RESULTS AND DISCUSSION

Synthesis and Structure. The *P,S*-Ru(II) complex **1** was previously prepared by dechlorination of $Ru(bpy)_2Cl_2$ with silver tetrafluoroborate followed by addition of 3′-(diphenylphosphino)-2,2′:5′,2″-terthiophene (PT_3) and precipitation of the product as a hexafluorophosphate salt. The brown $[Ru(bpy)_2PT_3\text{-}P,C](PF_6)$ complex (**2**) was obtained by reaction of **1** with base. Initially, we attempted to prepare the corresponding Os complexes using the same route, but the poor solubility of the $(NH_4)_2OsCl_6$ starting material prevented successful isolation of the product **3**. Variation of the volume of solvent used, the time at reflux, and deletion of the filtering step did not help, and in all cases we were unsuccessful in isolating the desired Os analogue of **1**. Meyer and co-workers have previously reported that the use of Ag salts for dechlorination of Os complexes does not work well, and recommended heating the metal precursor and ligand together in high boiling solvents such as glycerol or ethylene glycol.[21] In our hands, this method yielded only a small amount of the desired product along with multiple other products, including the monochloro species according to mass spectroscopic analysis. Longer heating at reflux (up to 5 days) did not improve the yield. Further modifications to the conditions established that using a solvent mixture of ethanol and water, in a two-to-one ratio, with extended (36−48 h) heating at reflux, gave the desired Os complex **3** in 42% yield (Scheme 1). The product was purified by column chromatography on neutral alumina. A similar procedure to that used to obtain **2** was employed to obtain the brown cyclometalated species $[Os(bpy)_2PT_3\text{-}P,C](PF_6)$, **4**, in 61% yield.

Single crystals of both complexes **3** and **4** were grown from solution, and solid state structures of both complexes were obtained (Figure 1). The bonding arrangement in both new

dx.doi.org/10.1021/ic200392n |*Inorg. Chem.* 2011, 50, 5113–5122

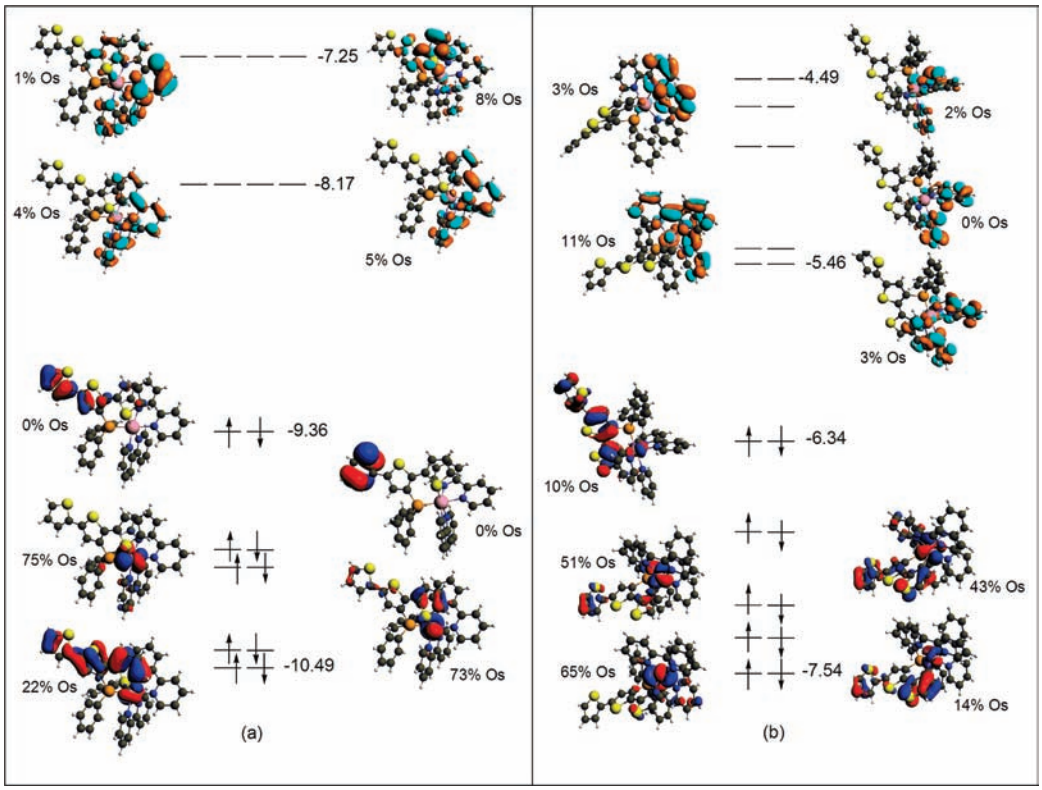

Figure 2. ADF-calculated plots of some frontier molecular orbitals (one of each spin−orbit pair shown, all $a_{1/2}$ in C_1 symmetry) for (a) **3** and (b) **4**, together with calculated energies (eV) for selected orbitals, electron occupations, and Mulliken metal atomic orbital percentages. The lowest energy orbital ($453a_{1/2}$ for both complexes) plot is lower left in both cases, alternating from one side to the other with increasing energy so that the HOMO plot is on the left side of the energy levels and the LUMO plot is on the right side of the energy levels in both cases.

structures is identical to that in the Ru analogues, and some differences in bond lengths and angles are observed (Supporting Information, Table S1). The $S_1-C_{36}-C_{37}-S_2$ torsion angle of 154.9(3)° in **3** is somewhat larger than in **1**. The larger torsion angle indicates increased coplanarity, resulting in increased π-orbital overlap between adjacent thienyl rings. In **3**, the bound thiophene ring is tilted away from the Os−S bond at an angle of 59.7°, slightly larger than the tilt angle in **1** (58.3°). The thiophene tilts away from the metal−sulfur bonds in these compounds to reduce unfavorable π^*-antibonding interactions between the thiophene and the metal.[22] The Os center may result in a greater degree of antibonding interaction, and consequently a larger tilt angle. The Os−C bond in complex **4** was found to be 2.095(3) Å, which is comparable to the metal carbon bond length in the Ru analogue, as are the other bond lengths. The $S_1-C_{36}-C_{37}-S_2$ torsion angle indicates the two locked thiophene rings in **4** are more coplanar than in **2**. The thiophene ring is almost coplanar with the vector of the Os−C bond (tilted 5.9°), a smaller tilt angle relative to the Ru analogue (7.3°). Here, the bound carbon is sp^2 hybridized, and the tilt angle suggests antibonding interactions may also play a role in these complexes.

Density Functional Theory (DFT) Calculations. Orbital plots for the Os(II) complexes together with their energies, electron populations, and calculated metal contributions are shown in Figure 2. Spin−orbit effects were included in the calculations so that all orbitals are listed as $a_{1/2}$ pairs. The results reveal many similarities in bonding between the corresponding Ru and Os complexes (orbital plots for the Ru analogues shown in Supporting Information, Figures S5 and S6). In comparing the corresponding PT_3-*P,S* and PT_3-*P,C* complexes, it is found that for the two *P,S* complexes both the highest occupied molecular orbital (HOMO) and the HOMO-1 have no metal contributions while the *P,C* complexes have minor metal character for the HOMO (3% Ru for **2** and 10% Os for **4**) and nearly equal metal and PT_3 contributions for the HOMO-1 (56% Ru for **2** and 43% Os for **4**).

DFT calculations on all four complexes indicate that the total metal bond order calculated by five different methods (Mayer, Gophinatan−Jug, and three Nalejawski−Mrozek definitions) is greater by about 0.6 for **3** vs **1** and **4** vs **2**, indicating stronger overall M−L bonding in the Os complexes compared to the corresponding Ru complexes. The increase in the total metal bond orders of 0.3 for both **2** vs **1** and **4** vs **3** indicates stronger overall M−L bonding in the *P,C* coordination mode where the PT_3 ligand is formally deprotonated, compared to the *P,S* mode where the ligand is formally uncharged. This is not surprising given the lower positive charge in complexes **2** and **4** which arises because of a negative formal charge on the coordinated C atom in the deprotonated PT_3 ligand. The significantly larger M−C bond orders for **2** and **4** compared to **1** and **3** are consistent with this conclusion. There is little difference in the calculated M−P and M−N (N *trans* to P) bond orders between complexes **1** and **2**, and between complexes **3** and **4**. The values of the total metal bond orders are provided in Supporting Information, Table S3 and range from 4.2 ± 0.4 for **1** to 5.0 ± 0.5 for **4** depending on the method used to calculate them.

The Hirshfeld, VDD, Mulliken, and MDC-q methods of calculating atomic charges on the metals all result in higher

dx.doi.org/10.1021/ic200392n |*Inorg. Chem.* 2011, 50, 5113–5122

positive charges by 0.1−0.2 for **1** vs **3** and **2** vs **4**, while the opposite is found with the AIM and NPA methods (Supporting Information, Table S4). The higher metal atomic charges for the Ru complexes compared to the corresponding Os complexes calculated by all but the AIM and NPA methods are consistent with a slightly higher electronegativity for Os compared to Ru,[23] and in fact the electronegativity equalized charges[24] calculated for the Ru complexes are higher by 0.1 than those for the corresponding Os complexes. All six ADF methods of calculating atomic charges on the metals show an increase in positive charge for **2** vs **1** and **4** vs **3**. The unexpectedly larger charges for the complexes with the *P,C* coordination mode suggest greater M-bpy π back-bonding and/or less bpy-M σ donation compared to those with the *P,S* mode. The more negative charges on the N atom trans to the coordinated C atom in **2** and **4** compared to those for the N atom trans to the coordinated S atom in **1** and **3** are consistent with this conclusion. The longer M−N bond distances for the N atom trans to C in **2** and **4** (2.15 and 2.12 Å, respectively) compared to the M−N bond distances for the N atom trans to S in **1** and **3** (2.07 Å for both complexes) suggests less bpy−M σ donation in **2** and **4** compared to **1** and **3**.

Cyclic Voltammetry. The cyclic voltammogram of **3** (Supporting Information, Figure S7a) shows a quasi-reversible oxidation peak at 1.23 V vs SCE, ~ 0.25 V lower than the first oxidation peak of **1**. ADF-calculated Mulliken AO contributions indicate that both the HOMO and HOMO-1 orbitals of **1** and **3** are completely localized on the PT_3 ligand. The first reduction peak of **3** occurs at −1.36 V vs SCE and is irreversible. This reduction is presumably localized on the bpy ligands, consistent with ADF calculations that reveal neither the lowest unoccupied molecular orbital (LUMO) nor the LUMO+1 have more than a 5% Os AO contribution. The cyclic voltammogram of **4** (Supporting Information, Figure S7b) shows two reversible waves, at 0.28 and 0.95 V vs SCE. Some small features are observed in the voltammogram and are attributed to products resulting from scanning over the full potential range. For **4**, the ADF-calculated HOMO is about 90% PT_3 localized while the HOMO-1 (0.48 eV lower in energy) is nearly equally distributed between the Os and PT_3 units, suggesting the oxidation wave at 0.28 V to be PT_3-localized and the 0.95 V oxidation wave to be due to removal of an electron from a mixed Os-PT_3 orbital. These assignments differ from those previously reported for the Ru analogues.[15] The earlier assignments were based only on the observation of small shifts in potential with methyl substitution on the PT_3. The oxidation potential of 0.95 V for **4** is 0.16 V lower than the corresponding value for **2** and is consistent with the smaller calculated atomic charge for the metal in **4** relative to **2**. In addition, **4** has reduction waves at −1.45 and −1.75 V vs SCE, both presumably corresponding to bpy-based processes as indicated by the ADF-calculated AO parentages for the LUMO and LUMO+1. These values are 0.08 and 0.03 V less negative, respectively, than the corresponding values for **2** and are consistent with the 0.06 V lower calculated LUMO energy for **4** versus **2**. The substantial decrease in the $Os^{2+/3+}$ oxidation potential between **3** and **4** is consistent with the lower energy of the mixed metal−ligand to ligand charge transfer transition (MLL′CT) transition (see below). A similar reduction in the $Ru^{2+/3+}$ oxidation potential was also observed between complexes **1** and **2**,[14] and can be accounted for at least in part by the reduction in overall charge from +2 for **1** and **3** to +1 for **2** and **4**.

Ground State Absorption Spectra. The UV−vis absorption spectra of the Os complexes in CH_3CN are shown in Figure 3,

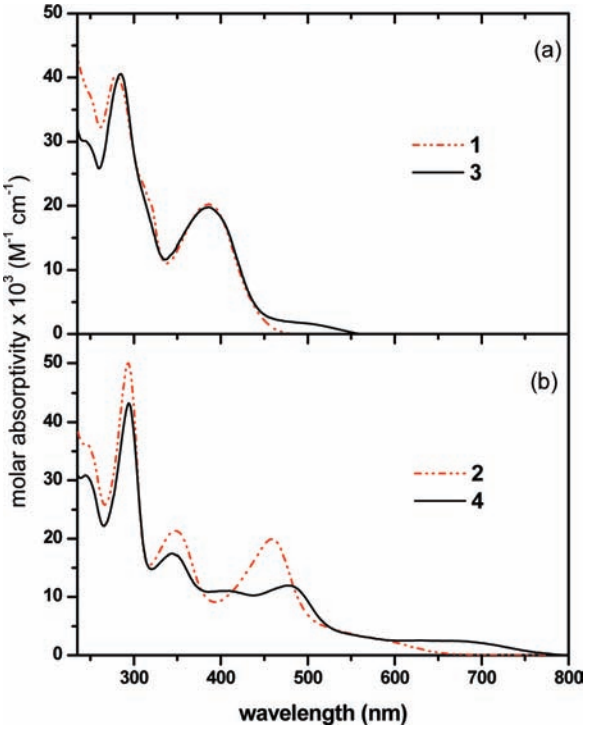

Figure 3. UV−vis absorption spectra of (a) $[Ru(bpy)_2PT_3$-*P,S*$]$ $(PF_6)_2$ (**1**), $[Os(bpy)_2PT_3$-*P,S*$]$ $(PF_6)_2$ (**3**) and (b) $[Ru(bpy)_2PT_3$-*P,C*$]$ (PF_6) (**2**) and $[Os(bpy)_2PT_3$-*P,C*$]$ (PF_6) (**4**) in CH_3CN.

along with the spectra of the Ru analogues for comparison. The absorption spectrum of complex **3** contains two major bands, a band at 286 nm assigned to the $\pi \rightarrow \pi^*$ transition of the bipyridine group, and a lower energy band with λ_{max} = 394 nm. The low energy band is shifted only very slightly from the corresponding band in the spectrum of **1**, similar to observations of the spectra of tris(bipyridine) metal complexes, where the ^{1}MLCT band in $[Ru(bpy)_3]^{2+}$ has λ_{max} = 451 nm[25] and λ_{max} = 450 nm in $[Os(bpy)_3]^{2+}$ with the ^{3}MLCT band observed between 520 and 700 nm.[26] This lower energy band in **1** was assigned to a charge transfer transition involving a mixed metal/terthiophene HOMO and bipyridyl based LUMO (a ^{1}MLL′CT transition).[15,16] ADF calculations for **1** and **3** indicate that the HOMO and HOMO-1 have no metal atomic orbital contributions, whereas the HOMO-2, -3, and -4 orbitals all contain substantial metal contributions and all lie within about 1 eV of the HOMO in energy. Therefore for both **1** and **3** the broad, overlapping absorption bands above 350 nm are likely to contain orbital contributions from both PT_3-localized and M-PT_3 delocalized orbitals and are best considered as ^{1}MLL′CT bands. Similarly, the broad band between 450 and 575 nm in the spectrum of **3** is assigned as a ^{3}MLL′CT transition based on the ADF calculations, increased in intensity relative to the Ru analogue because of the larger spin−orbit coupling in Os. In **1**, the shoulder at 320 nm was assigned to the terthienyl $\pi \rightarrow \pi^*$ transition. This blue-shifts in **3**, and is almost completely hidden under the bpy transition, and a small shoulder can be seen at ~300 nm.

The spectra of *P,C* complexes **2** and **4** contain more peaks than the corresponding *P,S* complexes **1** and **3**. The high energy peaks (λ < 375 nm, assigned to bpy and terthienyl based $\pi-\pi^*$ transitions) do not shift much between **2** and **4**. A band at

dx.doi.org/10.1021/ic200392n |*Inorg. Chem.* 2011, 50, 5113–5122

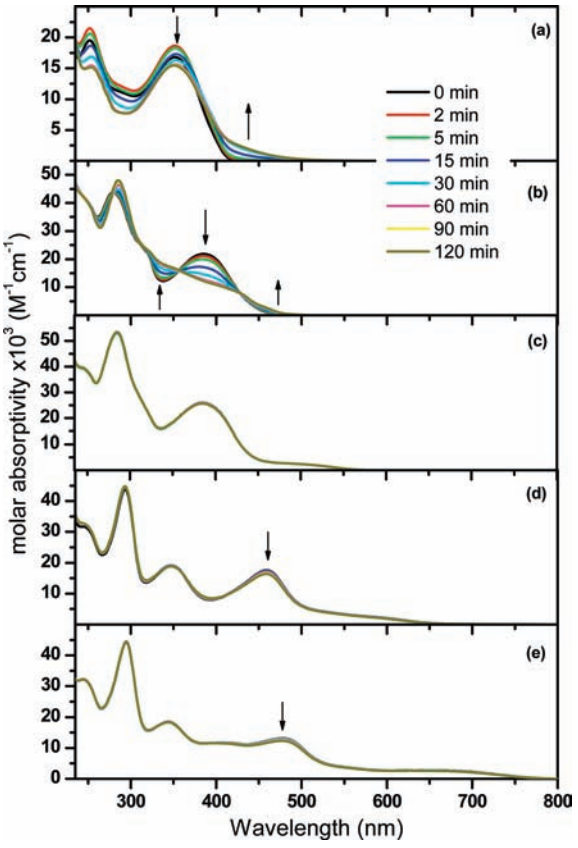

Figure 4. UV−vis spectra of (a) PT_3, (b) **1**, (c) **3**, (d) **2**, and (e) **4** in CH_3CN after 0, 2, 5, 15, 30, 60, 90, and 120 min of irradiation at 366 nm.

400 nm is observed in the spectrum of **4** which is not present in the spectrum of **2**; it is not clear what the origin of this new peak is. The charge transfer transition in **4** is red-shifted relative to the corresponding band in **2**. The ^{3}MLL′CT transition, that ADF calculations suggest corresponds to a HOMO and/or HOMO-1 to LUMO transition, red shifts to 650 nm, with the addition of a new shoulder at 560 nm. This red shift is consistent with the lower calculated atomic charge on the metal in **4** relative to that in **2**. There is a significant red-shift of the terthienyl band between the *P,S* and *P,C* complexes because of either the increased planarity of the thiophene rings in the *P,C* bound complexes or the change in the charge of the PT_3 ligand accompanying the orthometalation to form the *P,C* derivatives.

Photostability studies of PT_3 and the complexes in CH_3CN were carried out by extended irradiation with 366 nm light, using UV/vis spectroscopy as a tool to probe stability. Irradiation of PT_3 resulted in a decrease in the main absorption bands, and the growth of a low energy shoulder at ∼450 nm (Figure 4a). Previous studies have shown that irradiation of 2,2′:5′2″-terthiophene (T_3) with UV light results in polymerization to give longer oligomers.[27] The low energy absorption band observed upon irradiation of PT_3 is consistent with oligomerization of the terthiophene, resulting in a red shift in the absorption band. Irradiation of complexes **2**, **3**, and **4** under the same conditions results in only very small changes to the UV/vis spectra (Figure 4c−e), indicating that these complexes are all photostable under the irradiation conditions. On the contrary, irradiation of complex **1** results in substantial changes in the UV/vis spectrum (Figure 4b), demonstrating that this complex is not photostable under these conditions in solution. Although a small low energy shoulder also appears in this experiment, the higher energy region shows different changes than observed when PT_3 is irradiated, suggesting that different products are formed in the case of **1**. Mass spectroscopic analysis of a solution of photo-irradiated **1** suggests that a bipyridyl group is being lost during the irradiation process. This has been observed before in other photoactive metal bipyridyl complexes.[28] The photostability of the complexes did not change when irradiated under nitrogen or oxygen. Decomposition reactions of other metal bipyridyl complexes have been observed when MC states are accessible.[29] The increased photostability of the *P,C* bound species may be due to the reactive MC state lying higher in energy because of the coordination of the formally anionic ligand. The higher photostability of the Os complex **3** may also be due to a higher barrier to the MC state, since the lowest energy CT excited state in this complex is lower in energy than in **1**.

Emission Spectra. PT_3 has a short-lived emission centered at 435 nm (Table 1), attributed to radiative decay of the singlet $\pi-\pi^*$ state. Complexes **1** and **2** were previously reported to be either non-emissive or very weakly emissive upon excitation with visible light.[15] However, when excited at 355 nm, complex **1** exhibited short-lived emission at 430 nm.[30] The Os analogue **3** showed dual emission, with bands at 447 and 640 nm. Dual emission from metal complexes is unusual, but has been previously observed in some cases.[31] In both **1** and **3**, the lifetime of the species giving rise to the higher energy band is not sensitive to the presence of oxygen. The lifetime of the species giving rise to the lower energy band in **3** is significantly shorter in oxygen sparged solution. On the basis of these observations, the higher energy band in both **1** and **3** is assigned to emission from a terthiophene-localized singlet state. In **3**, enhanced intersystem crossing because of the heavier Os center also populates either a ^{3}MLL′CT or ^{3}LL′CT state which emits at lower energy, and has a longer lifetime. In complexes **2** and **4**, two emission bands are also observed. In the presence of O_2 the lower energy band becomes very weak in these complexes, and in **4** the lifetime is shorter in the presence of oxygen, supporting the assignment of this band to a triplet emission. Despite careful efforts to purify the complexes, the possibility of the higher energy emission band arising from free ligand cannot be entirely ruled out. However, emission of PT_3 occurs with λ_{max} = 435 nm, and the higher energy emission band observed in all the complexes is shifted from this maximum. Quantum yields were obtained for the lower energy emission band, and are comparable to those reported for related Os and Ru complexes.[32,33] Values were calculated for the radiative (k_r) and nonradiative (k_{nr}) decay constants and show the nonradiative decay dominates. Exciting complexes **1**−**4** at longer wavelengths resulted in only the lower energy emission being observed.

Transient Absorption. Transient absorption (TA) spectroscopy uses an excitation pulse to promote a fraction of molecules into the excited state and measures the difference in absorption between the ground state and excited state. The bands in a TA spectrum indicate an excited state absorption, while bleaches are due to stronger ground state absorptions than that of the excited state. The TA spectrum of PT_3 is shown in Figure 5. This spectrum shows a transient species absorbing between 400 and 600 nm, with a lifetime of 9 μs under N_2, that is quenched under O_2. Excitation of T_3 also results in a species with a similar, but sharper, absorbance from 400 to 600 nm with a 2.8 μs lifetime (Supporting Information, Figure S8). Under oxygen, the TA

dx.doi.org/10.1021/ic200392n |*Inorg. Chem.* 2011, 50, 5113–5122

Table 1. Photophysical Data for PT_3 and Complexes 1−4

		τ_{em}[a]		τ_{TA}[a]						
compound	λ_{em}[a]	N_2 sparged	O_2 sparged	N_2 sparged	O_2 sparged	Φ_{em}[a]	$k_r \times 10^{-4}$ (s^{-1})[b]	$k_{nr} \times 10^{-4}$ (s^{-1})[c]	$E_{1/2\ ox} \pm 0.01$ V vs SCE	$E_{1/2\ red} \pm 0.01$ V vs SCE
PT_3	435 nm	<0.05 ns	<0.05 ns	9 μs					1.30[d,e]	
1	430 nm	0.2 ns	0.1 ns	100 ns	35 ns				1.48[d]	−1.28[d]
2	423 nm	2 ns	1.5 ns	20 ns	10 ns				0.57	−1.53
	730 nm	8 ns	7 ns			0.0001	1.9	58.6	1.11	−1.78
3	447 nm	<0.05 ns	<0.05 ns	800 ns	70 ns					
	640 nm	170 ns	30 ns			0.003	1.1	399	1.23	−1.36
4	419 nm	1.8 ns	1.5 ns	2 ns	2 ns				0.28	−1.45
	640 nm	25 ns	10 ns			0.0002	1.5	1249	0.95	−1.75

[a] λ_{ex} = 355 nm, CH_3CN. [b] Calculated using $k_r = \Phi_{em}\tau_{em}^{-1}$. [c] Calculated using $k_{nr} = \tau_{em}^{-1} - k_r$ using N_2 sparged emission lifetimes. [d] Irreversible wave, E_p reported. [e] Reference 34.

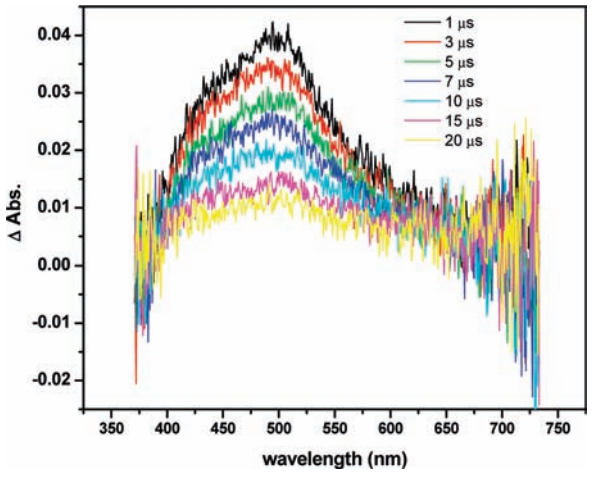

Figure 5. Time-resolved transient absorption spectra of PT_3 in CH_3CN. λ_{ex} = 355 nm.

spectrum of T_3 is also quenched. These data are consistent with the TA of both T_3 and PT_3 being due to a triplet−triplet excitation localized on the π system.

Excitation of **1** results in a broad TA with two overlapping bands between 400 and 700 nm (Figure 6a). The species decays with a lifetime of 100 ns in nitrogen-sparged acetonitrile, which is significantly reduced with oxygen sparging (Table 1). Complex **3** also shows an intense, broad TA with two bands between 450 and 725 nm (Figure 6b). In addition, there is a bleach centered at 400 nm. Both the absorptions and the bleach decay with a lifetime of 800 ns, which decreases in the presence of oxygen. The TA spectra of **1** and **3** resemble the TA spectrum of PT_3, although slightly red-shifted. In addition, no absorption due to a bipyridyl anion is seen at ~375 nm,[35] suggesting that the excited state of **1** and **3** observed in the TA spectra does not have metal-to-bipyridyl or thiophene-to-bipyridyl charge transfer character. Even at short times following excitation, the TA spectra do not show features associated with an MLL′CT state. The dependence of the lifetime and intensity of these bands on the presence of oxygen supports the conclusion that these are due to a triplet state, and the similarity of the TA spectra to that of PT_3 suggests that a PT_3 ligand-centered triplet state (^{3}LC) is being observed. The lack of observable emission in **1** suggests

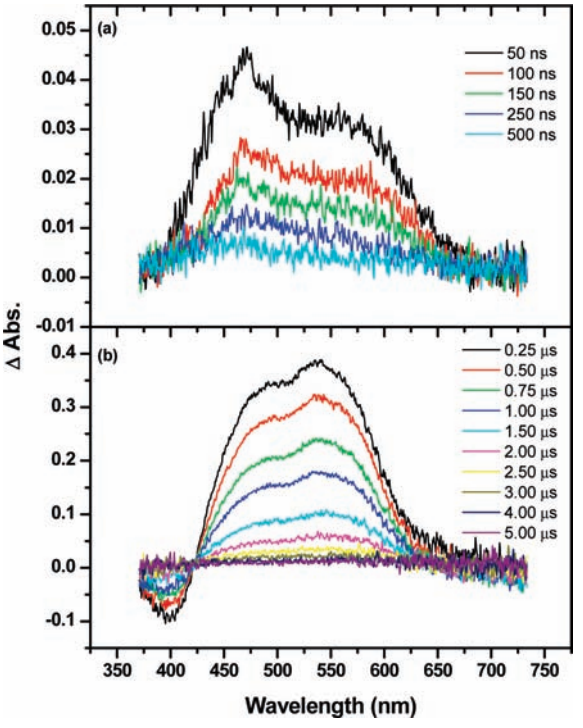

Figure 6. Time-resolved transient absorption spectra of (a) **1** and (b) **3** in CH_3CN. λ_{ex} = 355 nm.

that in this complex triplet energy transfer to the ^{3}LC state is very efficient. In complex **3**, weak emission attributed to decay of the ^{3}MLL′CT or ^{3}LL′CT state is observed, and the ^{3}LC state is still relatively efficiently populated and is the major species observed in the TA spectrum. The longer TA lifetime in **3** indicates that the ^{3}LC state must lie substantially lower in energy than the ^{3}MLL′CT and ^{3}LL′CT states, and these states are not in thermal equilibrium as has been observed previously in pyrene functionalized Ru diimine complexes.[36,37] In these cases the pyrene ^{3}LC state and Ru ^{3}MLCT states have the same lifetimes because of the equilibrium between them. The longer TA lifetime for **3** relative to **1** is attributed to the higher energy barrier to the MC state (see above), consequently this deactivation pathway is less prevalent in **3** than in **1**.

dx.doi.org/10.1021/ic200392n |*Inorg. Chem.* 2011, 50, 5113–5122

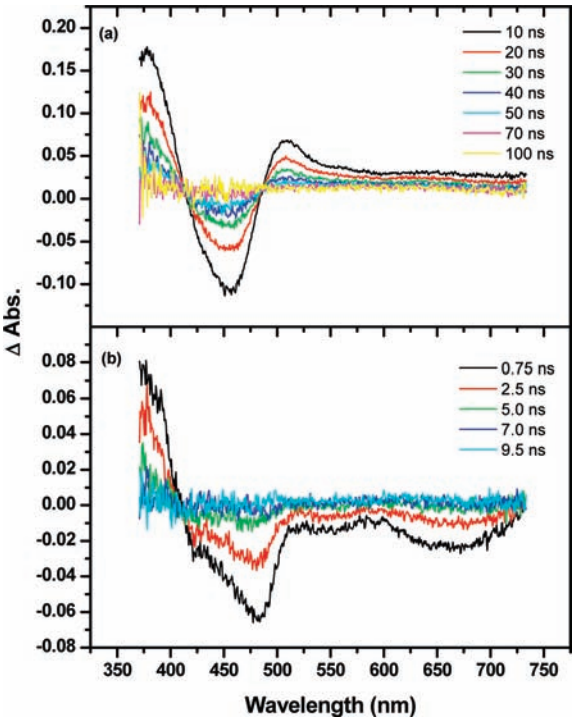

Figure 7. Time-resolved transient absorption spectra of (a) **2** and (b) **4** in CH_3CN. λ_{ex} = 355 nm.

Interestingly, the TA spectra of complexes **2** and **4** (Figure 7) are very different from the corresponding *P,S*-coordinated complexes **1** and **3**. Both **2** and **4** show an absorption at ~375 nm, and a bleach at ~450−475 nm. The TA spectrum of **2** also contains a broad, tailing absorption above 500 nm, while **4** shows a weak, broad bleach in this region. The TA of **2** decays monoexponentially with a lifetime of 20 ns under nitrogen, which decreases under O_2. The absorption at ~375 nm in the TA spectra of both **2** and **4** is assigned as a transition of the bpy^- anion based on comparison to related compounds.[35] The presence of this band indicates the observed excited state has charge transfer character. The lower energy absorption bands (>500 nm) in **2** are assigned to transitions of a cationic species having mixed-metal and ligand (PT_3) character. This assignment is based on several comparisons. The TA spectrum of T_3^+ shows an absorbance band between 530 and 545 nm,[38,39] and spectroelectrochemical studies on $\mathbf{2}^+$ have shown that this species has bands with absorption maxima at 558 and 632 nm.[40] Both these species have similar absorptions to the band observed in the TA spectrum of **2** at ~515 nm, suggesting a similar origin. An electron paramagnetic resonance (EPR) study of $\mathbf{2}^+$ showed that there is a significant metal contribution to the singly occupied molecular orbital (SOMO) in this oxidized complex.[16] This is consistent with ADF-calculations for **2** showing the HOMO-1 to have a 56% Ru contribution, but not with oxidation from the HOMO which has only a 3% Ru contribution. Taking all this data into account does not allow a conclusive assignment to be made of the cation, but a mixed parentage cation with both metal and PT_3 ligand character is most likely; thus, the observed excited state is characterized as a mixed metal−ligand to ligand CT (^{3}MLL′CT) state. The broad but very weak absorbance tail around 650 nm in **2** is characteristic of the presence of an anion,[41,42] cation,[43,44] or a charge transfer transition.[45] The TA

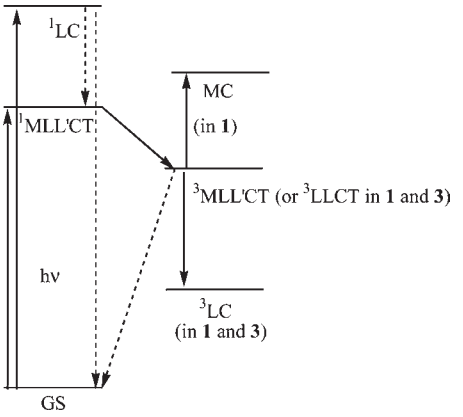

Figure 8. Qualitative energy diagram for **1**−**4**.

and emission lifetimes are similar for complex **2** suggesting that it is possible that these states are close in energy and in thermal equilibrium.

The excited state spectrum of complex **4** appears to be similar, with the clear presence of a transition assigned to the bpy anion. Transitions that could be assigned to a cation are not observed. Complex **4** absorbs to 700 nm, so the bleaching that is observed in the TA spectrum of this complex may hide weaker absorptions from a cationic species if these are present. The lifetime of this species is short, 2 ns under either nitrogen or oxygen. The measured lifetime is shorter than the emission lifetime, and it is possible that the weak TA spectrum introduces error and these states are also close in energy as in **2**. Other Ru and Os bipyridyl complexes show similar transient spectra. Excited state $Ru(bpy)_3^{2+}$ is reported to have absorption bands at 360 nm and above 525 nm, with a bleach centered at 440.[46] Excited state $Os(dmb)_3^{2+}$ has an absorption around 350 nm, and a strong bleach from 420 to 500 nm, with a weaker bleach extending past 650 nm.[47]

The photophysical results for complexes **1**−**4** can be summarized by consideration of the qualitative energy diagram shown in Figure 8. For the *P,S* bound complexes **1** and **3**, excitation results in simultaneous population of both ^{1}MLL′CT and ^{1}LC states on excitation at 355 nm. Some emission from the ^{1}LC is observed for both complexes. Internal conversion followed by intersystem crossing populates the ^{3}MLL′CT or ^{3}LL′CT state, from which some emission is observed for **3**. For **1**, the MC state lies close enough in energy to be thermally populated resulting in a photoreaction, and this does not occur in **3**. In both **1** and **3**, the ^{3}LC state is lower in energy than the ^{3}MLL′CT or ^{3}LL′CT state, resulting in triplet energy transfer and the observation of a transient species attributed to the ^{3}LC state. This coordination mode results in only a small perturbation in the electronic structure of the PT_3 ligand, possibly because of the weakly coordinated thiophene sulfur.

In the *P,C* bound complexes **2** and **4**, population of both ^{1}MLL′CT and ^{1}LC states occurs, and some emission from the ^{1}LC states is observed. Here, the ^{3}MLL′CT state is also populated, and emission from this state is observed.

CONCLUSIONS

Two new Os(II) complexes have been synthesized, characterized, and the photophysics compared to that of their Ru(II) analogues. Key differences that were observed were enhanced

dx.doi.org/10.1021/ic200392n |*Inorg. Chem.* 2011, 50, 5113–5122

photostability of the Os complexes, and a shift in the excited state observed by TA spectroscopy from a ^{3}LC triplet localized on the PT_3 group in the *P,S* complexes to a mixed metal−ligand to ligand CT state in the case of the *P,C* complexes. These results have important implications for the design of dyes for DSSCs and other related applications. In the *P,C* complexes the MLL′CT excited state involves charge transfer from the PT_3 localized HOMO to the bipyridyl localized LUMO. Adsorption of these complexes to nanostructured TiO_2 should allow charge injection from the LUMO and hole transport away from the metal center via the conjugated ligand. Studies are currently underway to probe the application of these complexes in DSSCs.

EXPERIMENTAL SECTION

General Procedures. All reactions were performed under N_2. The compounds *cis*-$Os(bpy)_2Cl_2$[48] and PT_3[49] were synthesized according to literature procedures. All other reagents were purchased from Aldrich and Strem and used as received. ^{1}H and $^{31}P\{^1H\}$ NMR spectra were collected on a Bruker AV-300 or AV-400 spectrometer and were referenced to residual solvent. ESI mass spectra were recorded on a Bruker Esquire-LC ion trap mass spectrometer equipped with an electrospray ion source. The solvent for the ESI-MS experiments was either methanol or dichloromethane/methanol and the concentration of the compound was ∼10 μM. High resolution mass spectra were recorded on a Waters Micromass LCT time-of-flight mass spectrometer equipped with an electrospray ion source. CHN elemental analyses were performed using an EA1108 elemental analyzer, using calibration factors. The calibration factor was determined by analyzing a suitable certified organic standard (OAS) of a known elemental composition. Cyclic voltammetry experiments were carried out on an Autolab PG STAT 12 potentiostat using a Pt working electrode, Pt mesh counter electrode and a silver wire reference electrode with 0.1 M $[(n\text{-}Bu)_4N]PF_6$ supporting electrolyte which was recrystallized 3 times from ethanol and dried under vacuum at 100 °C for 3 days. Decamethylferrocene (−0.125 V vs SCE in acetonitrile)[50] was used as an internal reference to correct the measured potentials with respect to saturated calomel electrode (SCE). UV−vis spectra were obtained on a Cary 5000 in HPLC grade solvent. Emission spectra were obtained on a PTI Quantamaster spectrometer. Transient absorption measurements and fluorescence lifetimes were carried out on an Princeton Instruments Spectra Pro 2300i Imaging Triple Grating Monochrometer/Spectrograph with a Hamamatsu Dynamic Range Streak Camera (excitation source: EKSPLA Nd:YAG laser, 35 ps pulse duration, λ = 355 nm). X-ray crystallographic data for molecules **3** and **4** were both collected on a Bruker X8 APEX II diffractometer using graphite monochromated Mo−Kα radiation, at −100 °C. Data were collected and integrated using the Bruker SAINT[51,52] software package. Data were corrected for absorption effects using the multiscan technique (SADABS).[53,54] Both structures were solved using direct methods[55] and all non-hydrogen atoms were refined anisotropically. All hydrogen atoms were placed in calculated positions. Molecule **3** crystallizes with two molecules of CH_2Cl_2 in the asymmetric unit. In **3** and **4** the terminal thiophene ring (containing S3) is disordered by a 2-fold rotation about the $C_{40}-C_{41}$ bond. The two ring fragments were modeled in both orientations using restraints to maintain reasonable ring geometries. All refinements were performed using the SHELXL-97[56] via the WinGX[57] interface.

Syntheses. *[Os(bpy)$_2$ PT$_3$-P,S] (PF$_6$)$_2$ (**3**).* PT_3 (0.164 g) was added to a degassed 2:1 EtOH-H_2O mixture containing $Os(bpy)_2Cl_2$ (0.200 g). The reaction mixture was heated to reflux under nitrogen with stirring for 48 h. The EtOH was removed in vacuo, and the remaining solution was added to aqueous ammonium hexafluorophosphate (1.136 g in 70 mL of H_2O) and stirred at room temperature for half an hour. The precipitate was filtered and washed with copious amounts of water and diethyl ether, and then dissolved in DCM and purified over neutral alumina. Once the brown band was eluted with DCM, acetone was used to elute the reddish-orange product band. The volume was reduced in vacuo, and the remaining solution was added to aqueous ammonium hexafluorophosphate (0.568 g in 30 mL of H_2O) and stirred at room temperature for half an hour. The precipitate was filtered and washed with copious amounts of water and diethyl ether to yield 181 mg (42%) of red solid. ^{1}H NMR (300 MHz, $CO(CD_3)_2$): δ 9.16 (d, J = 5.9 Hz, 1H), 8.96 (d, J = 5.7 Hz, 1H), 8.71 (d, J = 8.2 Hz, 1H), 8.67−8.60 (m, 3H), 8.23−8.02 (m, 5H), 7.70 (d, J = 5.7 Hz, 1H), 7.64−7.47 (m, 7H), 7.43−7.29(m, 6H), 7.23−7.16 (m, 3H), 7.11−7.05(m, 2H), 6.97 (d, J = 3.3 Hz, 1H), 6.87−6.81(m, 2H). $^{31}P\{^1H\}$ NMR (121 MHz, $CO(CD_3)_2$): δ −14.2 (s), −143.6 (septet, J_{PF} = 708 Hz, PF_6). m/z $[M - PF_6]^+$ 1080. Anal. $C_{44}H_{33}N_4S_3OsP_3F_{12}$ requires C, 43.14; H, 2.72; N, 4.57. Found C, 42.88; H, 2.99; N, 4.40%. HRMS (ESI) Calcd for $C_{44}H_{33}N_4F_6OsP_2S_3$: 1081.0845; Found: 1081.0862.

*[Os(bpy)$_2$PT$_3$-P,C] (PF$_6$) (**4**).* NaOH (0.20 g) was dissolved in degassed methanol (5 mL) to form a 1.0 M solution. Complex **3** (50 mg) was added and heated to reflux under nitrogen, with stirring, for 36 h. The solution was cooled to room temperature, and the MeOH was removed in vacuo. The precipitate was redissolved in 2 mL of MeOH. The dark solution was added dropwise to a solution of ammonium hexafluorophosphate (0.284 g) in H_2O (17 mL) and stirred at room temperature for half an hour. The precipitate was filtered and washed with copious amounts of water and diethyl ether and yielded 27 mg (61%) of dark brown solid. ^{1}H NMR (300 MHz, $CO(CD_3)_2$): δ 8.94 (d, J = 5.8 Hz, 1H), 8.57 (d, J = 8.2 Hz, 1H), 8.51−8.37 (m, 4H), 7.97(t, J = 7.8 Hz, 1H), 7.88−7.62 (m, 6H), 7.58−7.53(m, 1H), 7.43−7.35 (m, 6H), 7.18−7.02 (m, 4H), 6.95−6.81 (m, 4H), 6.65 (d, J = 2.7 Hz, 1H), 6.43 (t, J = 8.7 Hz, 2H), 6.20 (d, J = 4.9 Hz, 1H) $^{31}P\{^1H\}$ NMR (121 MHz, $CO(CD_3)_2$): δ −2.4 (s), −143.6 (septet, J_{PF} = 708 Hz, PF_6) m/z $[M - PF_6]^+$ 935. HRMS (ESI) Calcd for $C_{44}H_{32}N_4OsPS_3$: 935.1142; Found: 935.1155. Anal. $C_{44}H_{32}F_6N_4OsP_2S_3\cdot 2H_2O$ requires C, 47.38 ; H, 3.26; N, 5.03. Found C, 47.59; H, 3.11; N, 4.89%

X-ray Crystallography. **3**: Formula: $C_{46}H_{37}N_4S_3OsP_3F_{12}Cl_4$, M = 1394.89, Monoclinic, space group $P2_1/c$ (No. 14), Z = 4, a = 11.1984(8) Å, b = 20.8114(16) Å, c = 21.9881(17) Å, α = 90.0°, β = 91.752(4) °, γ = 90.0°, V = 5122.0(7) Å^3, T = 173 (1) K, 82845 reflections measured, 12304 unique (R_{int} =0.039), final R1($I > 2.00\sigma(I)$) = 0.037, wR2 ($I > 2.00\sigma(I)$) = 0.088. **4**: Formula: $C_{44}H_{32}N_4PS_3OsPF_6$, M = 1079.06, Monoclinic, space group $C2/c$ (No. 15), Z = 8, a = 39.8697(9) Å, b = 9.4270(2) Å, c = 28.1007(5) Å, α = 90°, β = 130.946(1) °, γ = 90°, V = 7977.5(3) Å^3, T = 173 (1) K, 56287 reflections measured, 9648 unique (R_{int} = 0.050), final R1($I > 2.00\sigma(I)$) = 0.030, wR2 ($I > 2.00\sigma(I)$) = 0.061.

Computational Methods. DFT calculations were performed with the 2009.01 version of the Amsterdam Density Functional (ADF) program.[58] Experimental X-ray crystallographic cation geometries (C_1 point group) were used for all four complexes. All calculations included scalar and spin−orbit relativistic effects through the zeroth-order relativistic approximation (ZORA),[59] except for bond orders and natural population analysis (NPA) atomic charges[60] which included only scalar relativistic effects. The generalized gradient approximation (GGA) approximation of DFT at the BP86 level was used in all cases,[58k,l] and all-electron (i.e., no frozen core approximation was applied) TZ2P basis sets from the ADF basis sets ZORA library were used for all atoms. Atomic charges on all atoms were calculated within ADF using the Voronoi (VDD),[61] Hirshfeld,[62] Bader atoms in molecule (AIM),[63] NPA, Mulliken, and multipole-derived quadrupole (MDC-q) methods. Bond orders were calculated within ADF using the Mayer, Gophinatan−Jug, and three Nalejawski−Mrozek methods N-M (1), N-M (2), and N-M (3) provided with the ADF program.[64]

dx.doi.org/10.1021/ic200392n |*Inorg. Chem.* 2011, 50, 5113–5122

■ ASSOCIATED CONTENT

Supporting Information. X-ray crystallographic data in CIF format for **3** and **4**, ^{1}H NMR spectra for **3** and **4**, selected bond lengths and angles for complexes **1**−**4**, cyclic voltammograms for **3** and **4**, TA spectra of T_3, ADF orbital plots of **1** and **2**, and tables of ADF-calculated total metal bond orders and metal atomic charges. This material is available free of charge via the Internet at http://pubs.acs.org.

■ AUTHOR INFORMATION

Corresponding Author
*E-mail: mwolf@chem.ubc.ca.

■ ACKNOWLEDGMENT

We thank the Natural Sciences and Engineering Research Council of Canada for funding, the Laboratory for Advanced Spectroscopy and Imaging (LASIR) for access to spectroscopic equipment, Dr. Saeid Kamal for assistance with the TA measurements. S.M. thanks NSERC, UBC, and the Walter C. Sumner Foundation for graduate fellowships.

■ REFERENCES

(1) Kalyanasundaram, K. *Photochemistry of Polypyridine and Porphyrin Complexes*, 1st ed.; Academic Press; London, 1992.
(2) Anderson, P. A.; Keene, F. R.; Meyer, T. J.; Moss, J. A.; Strouse, G. F.; Treadway, J. A. *J. Chem. Soc., Dalton Trans.* **2002**, 3820–3831.
(3) O'Regan, B.; Grätzel, M. *Nature* **1991**, *353*, 737–740.
(4) Liang, Y.; Feng, D.; Guo, J.; Szarko, J. M.; Ray, C.; Chen, L. X.; Yu, L. *Macromolecules* **2009**, *42*, 1091–1098.
(5) Howard, I. A.; Laquai, F.; Keivanidis, P. E.; Friend, R. H.; Greenham, N. C. *J. Phys. Chem. C.* **2009**, *113*, 21225–21232.
(6) Clarke, T. M.; Durrant, J. R. *Chem. Rev.* **2010**, *110*, 6736–6767.
(7) Walters, K. A.; Ley, K. D.; Cavalaheiro, C. S. P.; Miller, S. E.; Gosztola, D.; Wasielewski, M. R.; Bussandri, A. P.; van Willigen, H.; Schanze, K. S. *J. Am. Chem. Soc.* **2001**, *123*, 8329–8342.
(8) Meyer, T. J. *Pure Appl. Chem.* **1986**, *58*, 1193–1206.
(9) (a) Wong, C. T.; Chan, W. K. *Adv. Mater.* **1999**, *11*, 455–459. (b) Wong, W.-Y.; Wang, X.-Z.; He, Z.; Djurišić, A. B.; Yip, C.-T.; Cheung, K.-Y.; Wang, H.; Mak, C. S. K.; Chan, W.-K. *Nat. Mater.* **2007**, *6*, 521–527. (c) Wong, W.-Y.; Wang, X.-Z.; He, Z.; Chan, K.-K.; Djurišić, A. B.; Cheung, K.-Y.; Yip, C.-T.; Ng, A. M-C.; Xi, Y. Y.; Mak, C. S. K.; Chan, W.-K. *J. Am. Chem. Soc.* **2007**, *129*, 14372–14380. (d) Wong, W.-Y.; Ho, C.-L. *Acc. Chem. Res.* **2010**, *43*, 1246–1256. (e) Liu, L.; Ho, C.-L.; Wong, W.-Y.; Cheung, K.-Y.; Fung, M.-K.; Lam, W.-T.; Djurišić, A. B.; Chan, W.-K. *Adv. Funct. Mater.* **2008**, *18*, 2824–2833.
(10) Zhu, Y.; Millet, D. B.; Wolf, M. O.; Rettig, S. J. *Organometallics* **1999**, *18*, 1930–1938.
(11) Weinberger, D. A.; Higgins, T. B.; Mirkin, C. A.; Stern, C. L.; Liable-Sands, L. M.; Rheingold, A. L. *J. Am. Chem. Soc.* **2001**, *123*, 2503–2516.
(12) Zhu, S. S.; Swager, T. M. *Adv. Mater.* **1996**, *8*, 497–500.
(13) Higgins, T. B.; Mirkin, C. A. *Chem. Mater.* **1998**, *10*, 1589–1595.
(14) Moorlag, C.; Clot, O.; Wolf, M. O.; Patrick, B. O. *Chem. Commun.* **2002**, 3028–3029.
(15) Moorlag, C.; Wolf, M. O.; Bohne, C.; Patrick, B. O. *J. Am. Chem. Soc.* **2005**, *127*, 6382–6393.
(16) Moorlag, C.; Sarkar, B.; Sanrame, C. N.; Bäuerle, P.; Kaim, W.; Wolf, M. O. *Inorg. Chem.* **2006**, *45*, 7044–7046.
(17) Mayo, E. I.; Kilsa, K.; Tirrell, T.; Djurovich, P. I.; Tamayo, A.; Thompson, M. E.; Lewis, N. S.; Gray, H. B. *Photochem. Photobiol. Sci.* **2006**, *5*, 871–873.
(18) Bomben, P. G.; Robson, K. C. D.; Sedach, P. A.; Berlinguette, C. P. *Inorg. Chem.* **2009**, *48*, 9631–9643.
(19) Kober, E. M.; Meyer, T. J. *Inorg. Chem.* **1982**, *21*, 3967–3977.
(20) Balazs, G. C.; del Guerzo, A.; Schmehl, R. H. *Photochem. Photobiol. Sci.* **2005**, *4*, 89–94.
(21) Kober, E. M.; Caspar, J. V.; Sullivan, B. P.; Meyer, T. J. *Inorg. Chem.* **1988**, *27*, 4587–4598.
(22) Harris, S. *Polyhedron* **1997**, *16*, 3219–3233.
(23) Nagle, J. K. *J. Am. Chem. Soc.* **1990**, *112*, 4741–4747.
(24) Bratsch, S. G. *J. Chem. Educ.* **1984**, *61*, 588–590.
(25) Zhou, M.; Robertson, G. P.; Roovers, J. *Inorg. Chem.* **2005**, *44*, 8317–8325.
(26) Shaw, G. B.; Styers-Barnett, D. J.; Gannon, E. Z.; Granger, J. C.; Papanikolas, J. M. *J. Phys. Chem. A.* **2004**, *108*, 4998–5006.
(27) Huisman, C. L.; Huijser, A.; Donker, H.; Schoonman, J.; Goossens, A. *Macromolecules* **2004**, *37*, 5557–5564.
(28) Crutchley, R. J.; Lever, B. P. *Inorg. Chem.* **1982**, *21*, 2276–2282.
(29) Beeston, R. F.; Larson, S. L.; Fitzgerald, M. C. *Inorg. Chem.* **1989**, *28*, 4187–4189.
(30) A weak, very short-lived shoulder ∼500−525 nm is also observed in the emission spectra of **1**−**4**.
(31) (a) Siebert, R.; Winter, A.; Dietzek, B.; Schubert, U. S.; Popp, J. *Macromol. Rapid Commun.* **2010**, *31*, 883–888. (b) Wilson, G. J.; Launikonis, A.; Sasse, W. H. F.; Mau, A. W.-H. *J. Phys. Chem. A* **1997**, *101*, 4860–4866. (c) Song, L.-Q.; Feng, J.; Wang, X.-S.; Yu, J.-H.; Hou, Y.-J.; Xie, P.-H.; Zhang, B.-W.; Xiang, J.-F.; Ai, X.-C.; Zhang, J.-P. *Inorg. Chem.* **2003**, *42*, 3393–3395. (d) Tyson, D. S.; Luman, C. R.; Zhou, X.; Castellano, F. N. *Inorg. Chem.* **2001**, *40*, 4063–4071. (e) Lee, S. J.; Luman, C. R.; Castellano, F. N.; Lin, W. *Chem. Commun.* **2003**, 2124–2125.
(32) Fabian, R. H.; Klassen, D. M.; Sonntag, R. W. *Inorg. Chem.* **1980**, *19*, 1977–1982.
(33) Strouse, G. F.; Schoonover, J. R.; Dueding, R.; Boyde, S.; Jones, W. E., Jr. *Inorg. Chem.* **1995**, *34*, 473–487.
(34) Clot, O.; Wolf, M. O.; Patrick, B. O. *J. Am. Chem. Soc.* **2001**, *123*, 9963–9973.
(35) Sun, Y.; Liu, Y.; Turro, C. *J. Am. Chem. Soc.* **2010**, *132*, 5594–5595.
(36) Tyson, D. S.; Castellano, F. N. *J. Phys. Chem. A* **1999**, *103*, 10955–10960.
(37) Simon, J. A.; Curry, S. L.; Schmehl, R. H.; Schatz, T. R.; Piotrowiak, P.; Jin, X.; Thummel, R. P. *J. Am. Chem. Soc.* **1997**, *119*, 11012–11022.
(38) Evans, C. H.; Scaiano, J. C. *J. Am. Chem. Soc.* **1990**, *112*, 2694–2701.
(39) Emmi, S. S.; D'Angelantonio, M.; Beggiato, G.; Poggi, G.; Geri, A.; Pietropaolo, D.; Zotti, G. *Radiat. Phys. Chem.* **1999**, *54*, 263–270.
(40) Moorlag, C., Ph.D. Thesis, University of British Columbia, Vancouver, British Columbia, Canada, 2006.
(41) Aly, S. M.; Ho, C.-L.; Fortin, D.; Wong, W.-Y.; Abd-El-Aziz, A. S.; Harvey, P. D. *Chem.—Eur. J.* **2008**, *14*, 8341–8352.
(42) Haga, M.-A.; Ali, M. M.; Koseki, S.; Yoshimura, A.; Nozaki, K.; Ohno, T. *Inorg. Chim. Acta* **1994**, *226*, 17–24.
(43) Aly, S. M.; Ho, C.-L.; Wong, W.-Y.; Fortin, D.; Harvey, P. D. *Macromolecules* **2009**, *42*, 6902–6916.
(44) Zhang, L.-P.; Chen, B.; Wu, L.-Z.; Tung, C.-H.; Cao, H.; Tanimoto, Y. *Chem.—Eur. J.* **2003**, *9*, 2763–2769.
(45) Danilov, E. O.; Pomestchenko, I. E.; Kinayyigit, S.; Gentili, P. L.; Hissler, M.; Ziessel, R.; Castellano, F. N. *J. Phys. Chem. A* **2005**, *109*, 2465–2471.
(46) Wallin, S.; Davidsson, J.; Modin, J.; Hammarström, L. *J. Phys. Chem. A* **2005**, *109*, 4697–4704.
(47) Maubert, B.; McClenaghan, N. D.; Indelli, M. T.; Campagna, S. *J. Phys. Chem. A* **2003**, *107*, 447–455.
(48) Nakabayashi, Y.; Nakamura, K.; Kawachi, M.; Motoyama, T.; Yamauchi, O. *J. Biol. Inorg. Chem.* **2003**, *8*, 45–52.
(49) Clot, O.; Wolf, M. O.; Yap, G. P. A.; Patrick, B. O. *J. Chem. Soc., Dalton Trans.* **2000**, 2729–2737.

(50) Aranzaea, J. R.; Daniel, M.-C.; Astruc, D. *Can. J. Chem.* **2006**, *84*, 288–299.
(51) *SAINT*, Version 7.46A; Bruker AXS Inc.: Madison, WI, 1997–2007.
(52) *SAINT*, Version 7.60A; Bruker AXS Inc.: Madison, WI, 1997–2009.
(53) *SADABS*, Bruker Nonius area detector scaling and absorption correction, 2007/4; Bruker AXS Inc.: Madison, WI, 2007.
(54) *SADABS*, Bruker Nonius area detector scaling and absorption correction, 2008/1; Bruker AXS Inc.: Madison, WI, 2008.
(55) *SIR97*; Altomare, A.; Burla, M. C.; Camalli, M.; Cascarano, G. L.; Giacovazzo, C.; Guagliardi, A.; Moliterni, A. G. G.; Polidori, G.; Spagna, R. *J. Appl. Crystallogr.* **1999**, *32*, 115–119.
(56) Sheldrick, G. M. *SHELXL-97*, Programs for Crystal Structure Analysis, Release 97-2; Institüt für Anorganische Chemie der Universität Göttingen: Göttingen, Germany, 1998.
(57) *WinGX*, V1.70; Farrugia, L. J. *J. Appl. Crystallogr.* **1999**, *32*, 837.
(58) (a) Fonseca Guerra, C.; Snijders, J. G.; te Velde, G.; Baerends, E. J. *Theor. Chem. Acc.* **1998**, *99*, 391–403. (b) Fonseca Guerra, C.; Visser, O.; Snijders, J. G.; te Velde, G.; Baerends, E. J. In *Methods and Techniques for Computational Chemistry*; Clementi, E., Corongiu, G., Eds.; STEF: Cagliari, Italy, 1995; pp 305−395. (c) Baerends, E. J.; Ellis, D. E.; Ros, P. *Chem. Phys.* **1973**, *2*, 41–51. (d) Boerrigter, P. M.; te Velde, G.; Baerends, E. J. *Int. J. Quantum Chem.* **1988**, *33*, 87–113. (e) te Velde, G.; Baerends, E. J. *J. Comput. Phys.* **1992**, *99*, 84–98. (f) Snijders, J. G.; Baerends, E. J.; Vernooijs, P. *At. Data Nucl. Data Tables* **1981**, *26*, 483–509. (g) Krijn, J.; Baerends, E. J. *Fit Functions in the HFS Method*; Internal Report (in Dutch); Vrije Universiteit: Amsterdam, The Netherlands, 1984. (h) Slater, J. C. *Quantum Theory of Molecules and Solids*; McGraw-Hill: New York, 1974; Vol. 4. (i) Vosko, S. H.; Wilk, L.; Nusair, M. *Can. J. Phys.* **1980**, *58*, 1200–1211. (j) Becke, A. D. *J. Chem. Phys.* **1986**, *84*, 4524–4529. (k) Becke, A. *Phys. Rev. A* **1988**, *38*, 3098–3100. (l) Perdew, J. P. *Phys. Rev. B* **1986**, *33*, 8822–8824. ; Erratum: *Phys. Rev. B* **1986**, *34*, 7406. (m) Fan, L.; Ziegler, T. *J. Chem. Phys.* **1991**, *94*, 6057–6063. (n) Schipper, P. R. T.; Gritsenko, O. V.; van Gisbergen, S. J. A.; Baerends, E. J. *J. Chem. Phys.* **2000**, *112*, 1344–1352.
(59) (a) Chang, C.; Pelissier, M.; Durand, P. *Phys. Scr.* **1986**, *34*, 394–404. (b) van Lenthe, E.; Baerends, E. J.; Snijders, J. G. *J. Chem. Phys.* **1973**, *99*, 4597–4610. (c) van Lenthe, E.; van Leeuwen, R.; Baerends, E. J.; Snijders, J. G. *Int. J. Quantum Chem.* **1996**, *57*, 281–293.
(60) Glendening, E. D.; Badenhoop, J. K.; Reed, A. E.; Carpenter, J. E.; Bohmann, J. A.; Morales, C. M.; Weinhold, F. *NBO*, 5.0; Theoretical Chemistry Institute, University of Wisconsin: Madison, WI, 2001; http://www.chem.wisc.edu/~nbo5.
(61) Fonseca Guerra, C.; Handgraaf, J. W.; Baerends, E. J.; Bickelhaupt, F. M. *J. Comput. Chem.* **2004**, *25*, 189–210.
(62) (a) Hirshfeld, F. L. *Theor. Chim. Acta* **1977**, *44*, 129–138. For recent critical perspectives on this definition see:(b) Parr, R. G.; Ayers, P. W.; Nalewajski, R. F. *J. Phys. Chem. A* **2005**, 3957–3959. and(c) Bultinck, P.; Van Alsenoy, C.; Ayers, P. W.; Carbó-Dorca, R. *J. Chem. Phys.* **2007**, *126*, 144111 (1−9). (d) Mandado, M.; Van Alsenoy, D.; Mosquera, R. A. *J. Phys. Chem. A* **2004**, *108*, 7050–7055.
(63) (a) Rodriguez, J. L.; Bader, R. F. W.; Ayers, P. W.; Michel, C.; Gotz, A. W.; Bo, C. *Chem. Phys. Lett.* **2009**, *472*, 149–152. (b) Rodriguez, J. L.; Koster, A. M.; Ayers, P. W.; Santos-Vale, A.; Merino, G. *J. Comput. Chem.* **2009**, *30*, 1082–1092.
(64) Michalak, A.; DeKock, R. L.; Ziegler, T. *J. Phys. Chem. A* **2008**, *112*, 7256–7263, and references therein.